10-1-1995

LONG-PERIOD CEPHEIDS: MODELS AND OBSERVATIONS

Norman R. Simon
University of Nebraska - Lincoln, nsimon@unl.edu

Shashi M. Kanbur
University of Nebraska-Lincoln, kanbur@oswego.edu

THE ASTROPHYSICAL JOURNAL, 451:703–710, 1995 October 1

LONG-PERIOD CEPHEIDS: MODELS AND OBSERVATIONS

NORMAN R. SIMON AND SHASHI M. KANBUR[1]
Department of Physics and Astronomy, University of Nebraska, Lincoln, NE 68588-0111
Received 1995 February 13; accepted 1995 April 6

ABSTRACT

We compile a list of 50 long-period Cepheids ($12^d < P < 70^d$) with light curves suitable for Fourier decomposition. For $P > 20^d$, the plots versus period of the Fourier quantities ϕ_{21}, ϕ_{31}, ϕ_{41}, and R_{21} all show a slow rise, with considerable scatter. Hydrodynamic calculations are performed to model the observed stars. The theoretical light curves are converted from bolometric to visual, and the Fourier coefficients compared with the observed ones. While the theoretical values follow the observed trends in a crude, general sense, differences are noted. At the lower end of the period range the models depart systematically from the observed stars. At longer period, the differences are much less striking, perhaps being obscured by scatter in the observations. We conclude that a detailed comparison between theory and observation must await a more extensive and accurate sample of observed stars.

Subject headings: Cepheids — hydrodynamics — stars: oscillations

1. INTRODUCTION

Recent observations of Cepheids in the Virgo Cluster galaxies NGC 4571 (Pierce et al. 1994) and M100 (Freedman et al. 1994) comprise a vigorous start on the final process that will nail down the Hubble constant, H_0. The Cepheids monitored in these studies had periods which ranged from 20 to 90^d. Indeed, the extension of the primary distance scale to Virgo and beyond will depend upon observations made at the long-period end of the Cepheid sample. Unfortunately, it is just these long-period Cepheids which have been least studied, both observationally and theoretically.

In the present work, we construct a grid of hydodynamic pulsation models and compare their (theoretical) light curves with those of a large observational sample of Cepheids with $P > 12^d$. The method used is that of Fourier decomposition, where the light curves are fitted with a Fourier series, $A_0 + A_j \cos(jwt + \phi_j)$ [summation convention], and their shapes quantified in terms of combinations of the low-order coefficients, viz., $\phi_{j1} = \phi_j - j\phi_1$ and $R_{j1} = A_j/A_1$. We shall find that while the models crudely duplicate the observed runs of the Fourier coefficients, neither the calculations nor the observations are at present precise enough to determine fundamental parameters for the observed stars.

2. THE OBSERVATIONS

Table 1 lists in order of increasing period 50 Cepheids with $P > 12^d$. The first six columns give the star name and period, followed by the values of the Fourier quantities R_{21}, ϕ_{21}, ϕ_{31}, and ϕ_{41} as determined by Fourier decomposition (Simon & Lee 1981) of the V-magnitude light curves. The last column provides literature references as indicated in the footnote. The Pel data were converted from the Walraven to the Johnson system (using the prescription given by Pel 1976) before the Fourier technique was applied. The Cepheids are all galactic, except for five stars taken from the Saha et al. (1994) observations of IC 4182, the galaxy which contains the historical Type Ia supernova, 1937C. The Table 1 sample consists of all stars in the cited references whose light curves were deemed suitable for Fourier decomposition (see, e.g., Simon & Lee 1981; Simon & Moffett 1985).

In Figures 1–4, we plot versus period the Fourier terms ϕ_{21}, ϕ_{31}, ϕ_{41}, and R_{21}, respectively. The different symbols denote different observers as indicated in the captions. No set of observations stands out as distinct in these diagrams; this includes the data for the Cepheids in IC 4182 (see also Simon & Clement 1994). The sharp rise at short period in all the Fourier terms is due to the Population I Cepheid resonance near 10^d (Simon & Schmidt 1976; Simon & Lee 1981). Beyond 20^d, there is a slower rise with considerably more scatter. This is generally true of all the Fourier terms, except that the two stars of longest period break this trend by showing relatively small values of R_{21} (Fig. 4).

A number of correlations may be noted among the Fourier terms. Figures 5, 6, and 7 display plots of ϕ_{41} versus ϕ_{31}, ϕ_{31} versus R_{21}, and ϕ_{41} versus R_{21}, respectively. In all three plots, the quantities are seen to increase in tandem. This agrees with correlations found between ϕ_{31} and R_{21} among the RRc stars in ω Centauri (Simon 1990a), and between ϕ_{41} and ϕ_{31} in a group of galactic Cepheids of shorter period (Simon & Moffett 1985). In Figure 5, there are seven stars which stand out from the main trend. The five points which are below and the two above may be made to conform by increasing their values of ϕ_{41} in the former case and decreasing them in the latter. The same changes applied to these seven stars in the ϕ_{41} versus. R_{21} diagram (Fig. 7) are then seen to reduce the scatter in that figure significantly. Since the fourth-order Fourier term has the smallest amplitude of any treated here and is thus the most difficult to determine from the fit, it is not surprising that ϕ_{41} may be in error for a number of stars. This analysis hints that the trends in Figures 5–7 (and perhaps those in Figs. 1–4) may be considerably tighter than they appear in the present data.

3. THE MODELS

We constructed 33 hydrodynamic pulsation models using the code TGRID (Simon & Aikawa 1986) with OPAL opacities. The chemical composition was $X = 0.70$, $Z = 0.02$ and

[1] Current address: Department of Physics and Astronomy, University of Glasgow, Glasgow G12 8QQ, Scotland.

TABLE 1

FOURIER DECOMPOSITION PARAMETERS FOR LONG-PERIOD CEPHEIDS

Star	Period	R_{21}	ϕ_{21}	ϕ_{31}	ϕ_{41}	Reference
KK Cen	12.180	0.243	4.196	7.158	4.848	P
VX Cru	12.213	0.306	4.166	7.899	4.477	P
SS CMa	12.362	0.168	4.171	6.925	4.072	P
U Nor	12.641	0.179	4.211	7.300	4.461	P
SY Nor	12.645	0.166	4.183	7.277	5.272	P
SU Cru	12.848	0.252	3.806	7.593	5.875	P
Z Sct	12.901	0.166	4.604	7.572	5.262	MB
EX Vel	13.234	0.056	3.617	6.490	4.593	P
FI Car	13.454	0.010	4.199	6.711	4.675	P
VY Sgr	13.557	0.239	4.460	7.720	5.700	P
BN Pup	13.673	0.243	4.750	8.458	6.028	P
SZ Cas	13.638	0.212	4.012	8.254	5.132	MB
TT Aql	13.755	0.226	4.510	7.855	5.678	P
TX Cyg	14.710	0.254	4.417	7.978	5.796	MB
UZ Sct	14.744	0.159	4.234	7.436	5.604	P
RW Cas	14.792	0.223	4.549	7.762	5.803	MB
SZ Cyg	15.110	0.218	4.259	7.713	5.732	MB
SV Mon	15.233	0.240	4.585	8.019	5.972	MB
X Cyg	16.386	0.244	4.433	8.050	5.958	MB
RW Cam	16.415	0.227	4.336	7.716	5.538	MB
CD Cyg	17.074	0.270	4.306	8.295	6.226	MB
TX Cen	17.094	0.253	4.404	8.054	5.968	P
Y Oph	17.127	0.223	4.002	7.681	3.974	MB
SZ Aql	17.138	0.266	4.415	8.078	5.967	P
C4-V10	18.3	0.315	4.37	8.03	6.36	S
VY Car	18.921	0.271	4.468	8.042	6.165	P
RU Sct	19.704	0.316	4.381	8.517	6.580	P
RY Sco	20.316	0.320	4.086	8.524	6.705	P
WZ Sgr	21.850	0.299	4.545	8.336	6.428	MB
WZ Car	23.021	0.407	4.580	9.087	7.423	P
VZ Pup	23.164	0.402	4.460	8.906	7.234	P
C1 – V4	24.7	0.329	4.60	8.74	7.25	S
X Pup	25.961	0.411	4.512	9.318	7.576	P
T Mon	27.021	0.344	4.511	8.809	7.005	P
RY Vel	28.127	0.387	4.444	9.120	7.336	P
V609 Cyg	31.076	0.440	4.565	9.252	7.695	B
V396 Cyg	33.247	0.342	4.453	8.698	6.924	B
KN Cen	34.019	0.405	4.475	8.848	7.048	P
C4 – V8	35.2	0.395	4.78	9.37	8.59	S
L Car	35.533	0.315	4.400	8.641	6.956	P
C2 – V2	37.5	0.439	4.93	9.66	8.45	S
EV Aql	38.629	0.374	4.658	9.388	7.580	B
U Car	38.768	0.459	4.800	9.570	7.669	P
RS Pup	41.387	0.377	4.852	9.436	7.823	P
C1 – V6	42.0	0.432	4.70	9.62	7.94	S
SV Vul	45.024	0.426	4.667	9.379	7.664	B
V1467 Cyg	48.524	0.426	4.881	9.672	8.070	B
CE Pup	49.530	0.397	5.088	9.478	9.029	P
GY Sge	51.601	0.326	4.763	9.578	7.665	B
S Vul	68.003	0.291	4.952	9.778	8.290	B

REFERENCES.—P = Pel 1976; MB = Moffett & Barnes 1985; S = Saha et al. 1994; B = Berdnikov 1994.

convection was neglected. The model parameters had ranges: $5.5 \leq M \leq 12.0\ M_{\odot}$, $3.597 \leq \log L \leq 4.534$, and $5000 \leq T_e \leq 5600$. The bulk of these models followed the evolutionary relation (Chiosi 1989)

$$\log L = 3.61 \log M + 0.94\ , \quad (1)$$

but a few were also calculated according to (Becker, Iben, & Tuggle 1977)

$$\log \mathrm{L} = 3.68 \log M + 0.46\ . \quad (2)$$

Although more recent evolutionary tracks produce relations which differ somewhat from equations (1) and (2), we shall argue below that the Fourier coefficients of the theoretical light curves will be insensitive to such differences within the uncertainty caused by imprecision in the observations.

The bolometric light variations produced by TGRID were converted to visual magnitudes by employing a bolometric correction at each point on the light curve. These corrections came from Table 1 of Kurucz (1991). To determine the bolometric corrections as a function of temperature and gravity, we fit the Kurucz data in the range $3750 \leq T_e \leq 8000$ K, $0 \leq \log g \leq 5$ with the following expression

$$\mathrm{BC} = A_0 + A_1 \log T_e + A_2 (\log T_e)^2 + A_3 (\log T_e)^3 + A_4 \log g\ , \quad (3)$$

where $A_0 = -2427.959$, $A_1 = 1868.993$, $A_2 = -479.5952$, $A_3 = 41.02427$, and $A_4 = 0.01523420$. The standard deviation of this fit is 0.023 mag, and in the range $4000 \leq T_e \leq 8000$ K, equation (3) never departs from the tabulated values by more

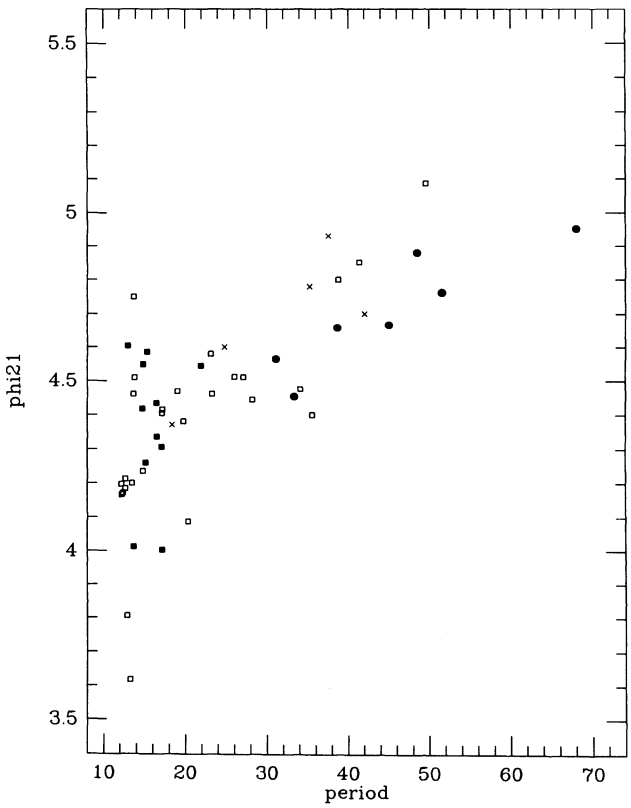

FIG. 1.—ϕ_{21} vs. period for observed stars. Symbols correspond to references in Table 1 as follows: *open squares*: P; *filled squares*: MB; *dots*: *B*; *crosses*: S.

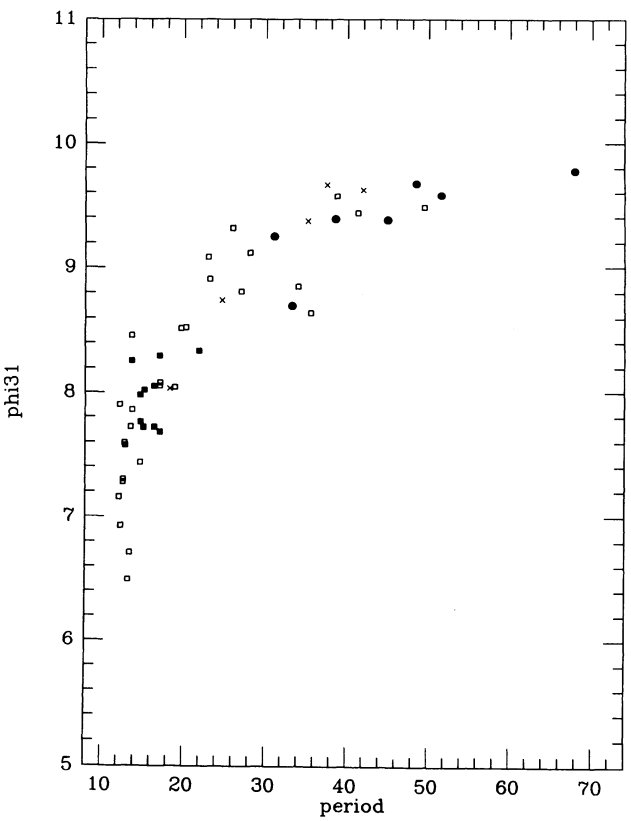

FIG. 2.—ϕ_{31} vs. period for observed stars. Symbols as in Fig. 1

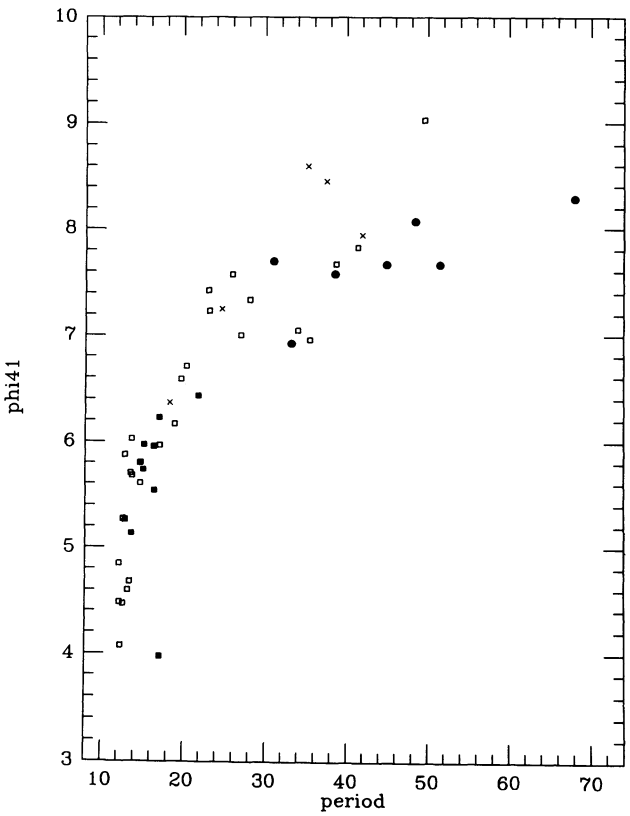

FIG. 3.—ϕ_{41} vs. period for observed stars. Symbols as in Fig. 1

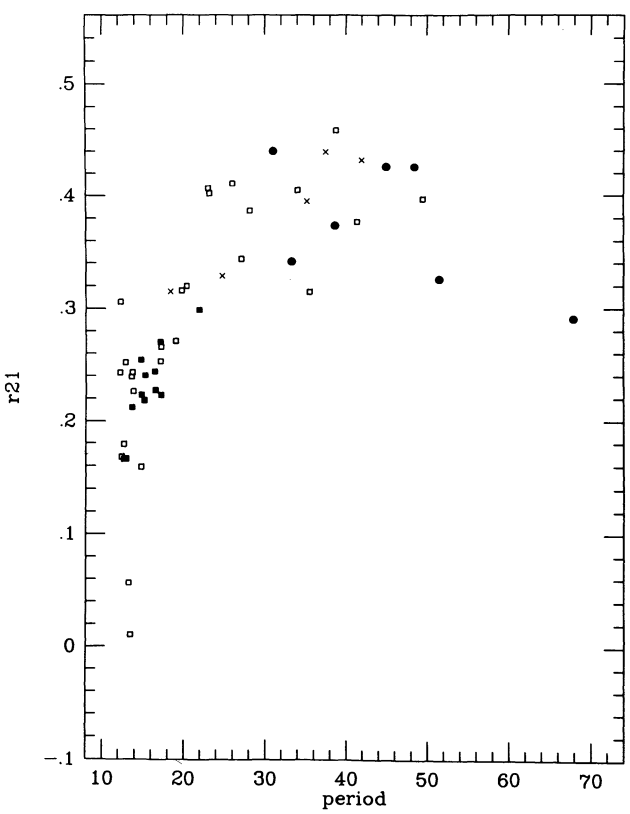

FIG. 4.—R_{21} vs. period for observed stars. Symbols as in Fig. 1

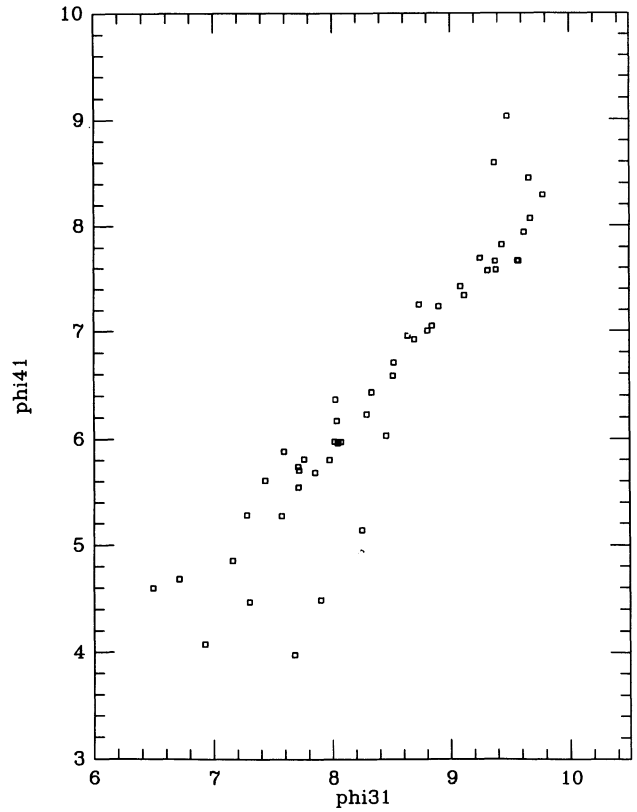

FIG. 5.—ϕ_{41} vs. ϕ_{31} for observed stars

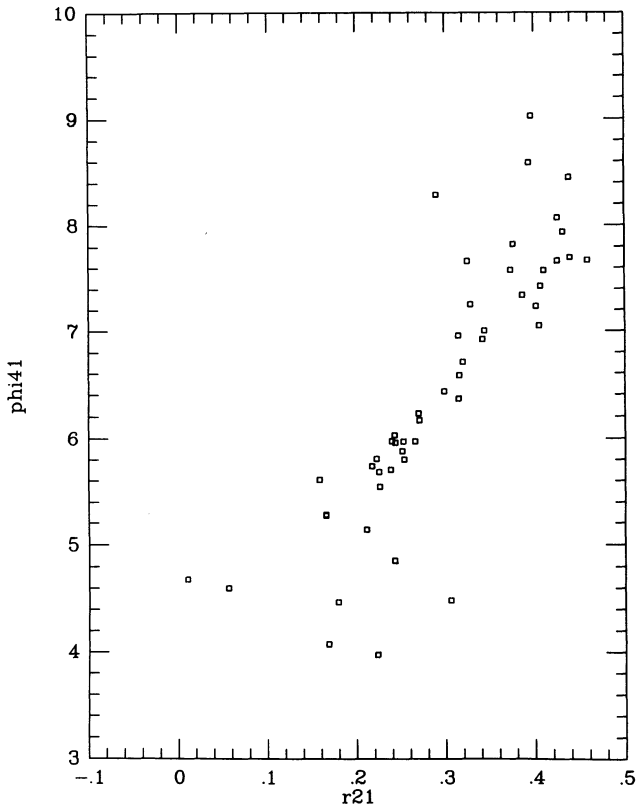

FIG. 7.—ϕ_{41} vs. R_{21} for observed stars

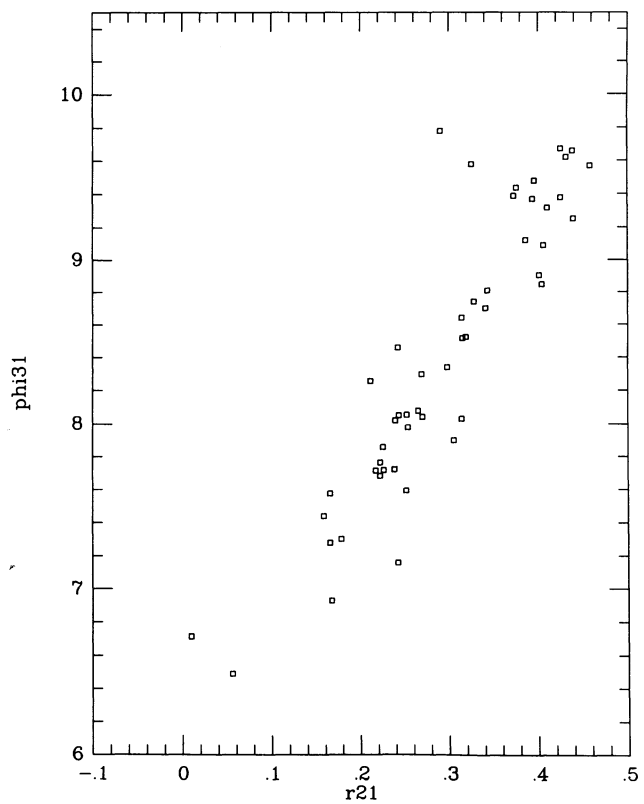

FIG. 6.—ϕ_{31} vs. R_{21} for observed stars

than 0.04 mag. This expression should not be used for temperatures below 4000 K or above 8000 K.

With the theoretical light curves, visual and bolometric, thus in hand, we subjected both sets to Fourier decomposition. For almost all models, the visual Fourier terms had values slightly lower than the bolometric. The average differences, bolometric minus visual, were 0.11, 0.19, 0.24, and 0.015 for ϕ_{21}, ϕ_{31}, ϕ_{41}, and R_{21}, respectively. These differences are of the same size but opposite sign to those given for a small number of cases by Simon & Moffett (1985). We beleve that the Simon-Moffett values were reported with incorrect sign.

Table 2 presents the model parameters along with the visual Fourier decomposition coefficients. In Figures 8–11 we plot versus period the runs of ϕ_{21}, ϕ_{31}, ϕ_{41}, and R_{21}, respectively, for the hydrodynamic visual light curves. The open squares represent the models constructed according to equation (1) and the filled squares according to equation (2). The point near 14^d occupies a unique position owing to the fact that the corresponding model happens to lie very close to the resonance $P_2/P_0 = 0.5$. The remainder of the filled squares do not depart dramatically from the open squares, except perhaps in Figure 11, where the R_{21} values corresponding to equation (2) seem generally smaller. In plots of ϕ_{41} versus ϕ_{31}, ϕ_{31} versus R_{21}, and ϕ_{41} versus R_{21} (none of them shown here), the two sets of models turn out to be virtually indistinguishable. In any event, given the scatter in the observational quantities (Figs. 1–4), we did not deem it useful to pursue such differences further. Recent evolutionary tracks indicate a slope of about 4.0 in the luminosity-mass relation, and a zero point perhaps somewhere in between those of equations (1) and (2) (Simon 1995). Once again, given the scatter in the observed data, the differences in

TABLE 2

HYDRODYNAMIC MODEL PARAMETERS

M	log L	T_e	P_0	R_{21}	ϕ_{21}	ϕ_{31}	ϕ_{41}
6.03.....	3.741	5461	14.36	0.309	4.46	8.82	6.38
6.03.....	3.741	5161	17.32	0.430	4.72	9.56	7.83
6.46.....	3.849	5404	17.75	0.357	4.49	8.97	6.92
6.46.....	3.849	5104	21.66	0.425	4.88	9.49	7.85
7.42.....	4.067	5293	27.35	0.422	4.45	9.19	7.63
7.42.....	4.067	5043	32.32	0.413	4.70	9.38	8.14
8.50.....	3.880	5243	17.16	0.241	4.45	9.01	5.52
8.50.....	3.880	5043	19.59	0.292	4.63	9.18	7.56
9.50.....	4.058	5143	24.46	0.404	4.62	9.26	7.13
8.00.....	3.783	5300	14.16	0.045	5.32	5.76	4.05
6.00.....	3.733	5600	12.99	0.230	4.32	8.04	5.90
6.00.....	3.733	5350	15.22	0.337	4.51	9.19	6.95
5.50.....	3.597	5350	12.24	0.233	4.59	9.07	5.71
5.50.....	3.597	5120	14.24	0.301	4.68	9.32	7.96
6.50.....	3.859	5470	17.25	0.318	4.40	8.76	6.74
6.50.....	3.859	5270	19.68	0.386	4.64	9.22	7.32
6.40.....	3.834	5500	16.29	0.299	4.40	8.68	6.56
6.40.....	3.834	5300	18.53	0.369	4.58	9.18	7.22
6.20.....	3.785	5370	16.34	0.339	4.50	9.03	6.82
6.20.....	3.785	5500	15.04	0.283	4.41	8.59	6.45
6.70.....	3.906	5450	18.91	0.330	4.41	8.91	6.76
6.70.....	3.906	5250	21.55	0.384	4.65	9.18	7.35
7.00.....	3.975	5400	21.84	0.355	4.41	9.04	7.02
7.00.....	3.975	5200	24.92	0.363	4.59	9.12	7.63
7.20.....	4.019	5400	23.48	0.370	4.40	9.09	7.09
7.20.....	4.019	5200	26.81	0.403	4.55	9.23	7.69
8.00.....	4.184	5200	35.23	0.480	4.57	9.50	8.19
9.00.....	4.369	5200	48.25	0.445	4.75	9.63	8.08
10.0.....	4.534	5100	69.02	0.436	5.07	10.38	9.39
10.0.....	4.140	5000	30.87	0.412	4.89	9.41	7.71
9.00.....	4.369	5100	51.76	0.494	4.82	9.87	8.39
11.0.....	4.292	5000	39.79	0.373	4.65	9.16	7.75
12.0.....	4.431	5000	50.39	0.495	4.63	9.55	8.07

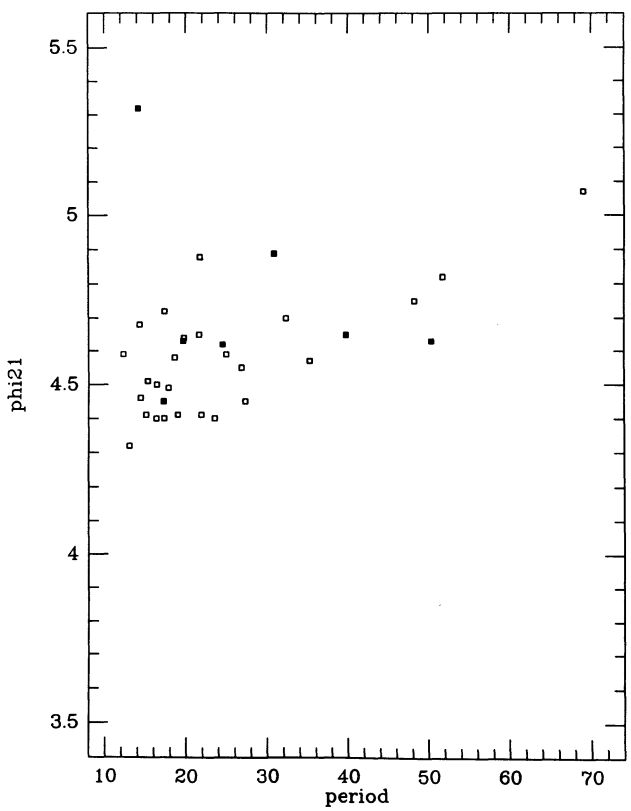

FIG. 8.—ϕ_{21} vs. period for models constructed according to eq. (1) (*open squares*) and eq. (2) (*filled squares*).

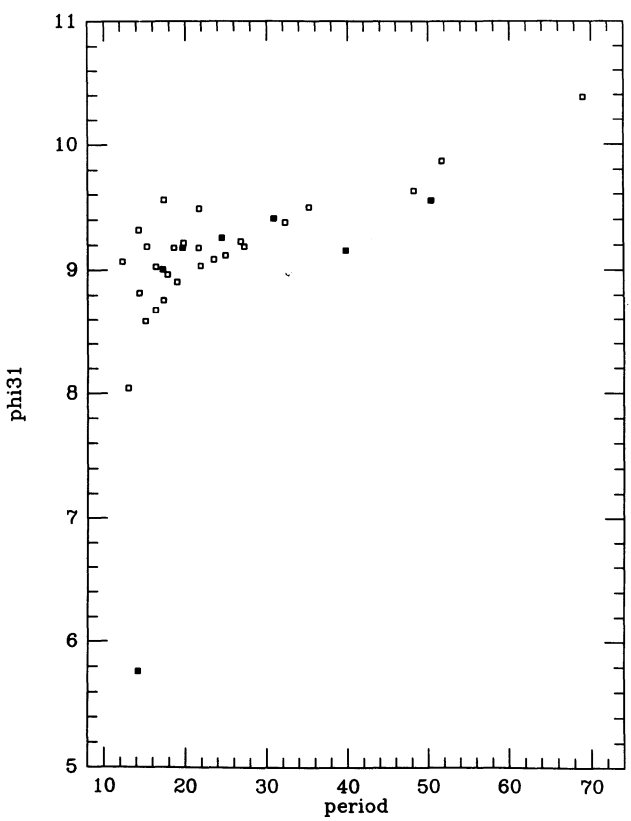

FIG. 9.—ϕ_{31} vs. period for models. Symbols as in Fig. 8

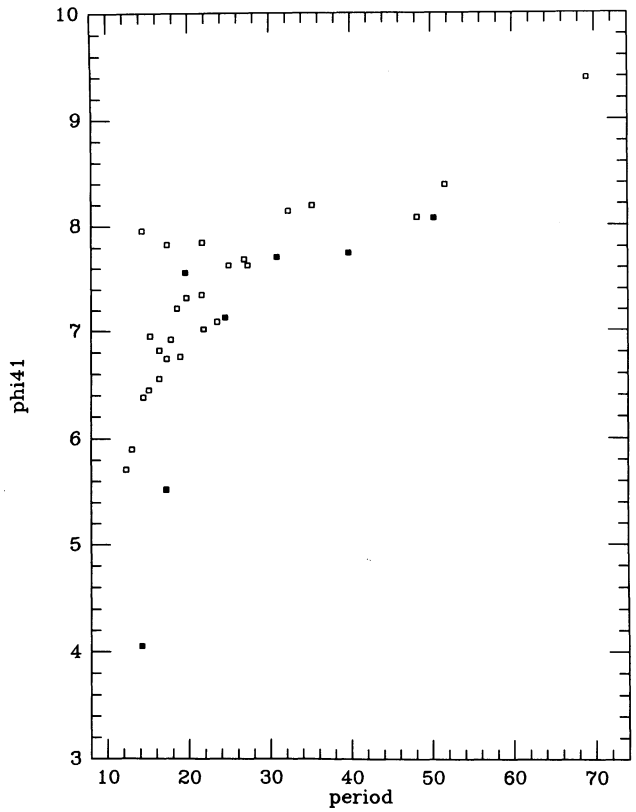

FIG. 10.—ϕ_{41} vs. period for models. Symbols as in Fig. 8

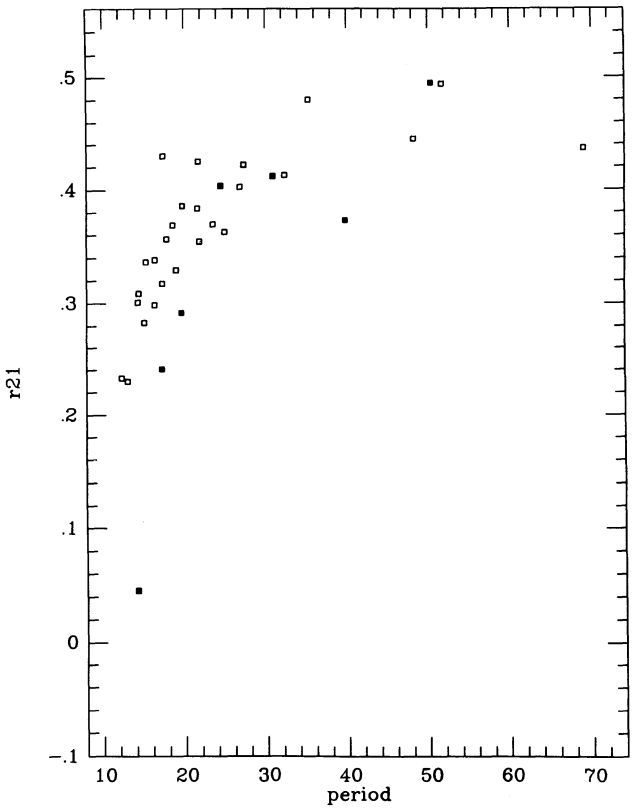

FIG. 11.—R_{21} vs. period for models. Symbols as in Fig. 8

the theoretical Fourier terms occasioned by different luminosity-mass relations are not likely to be significant in any current comparison between observation and theory.

4. THEORY VERSUS OBSERVATION

In Figures 12–15, we once more show plots of the Fourier quantities versus period. Here the filled squares represent the models (visual magnitudes) and the open squares the observed stars. In Figure 12, the two sets generally coincide, except that the models cannot reproduce observed light curves with ϕ_{21} values of less than about 4.5. In the period range from about 10^d to 30^d, the theoretical values of ϕ_{31} (Fig. 13) are systematically higher than those observed. At longer periods any differences are not so marked. Similar behavior may be noted in the ϕ_{41} plot displayed in Figure 14, while Figure 15 shows theoretical R_{21} values that tend to be larger than the observed quantities for all periods longer than about 15^d.

Recent studies comparing observed Cepheids with hydrodynamic pulsation models have been made by Buchler, Moskalik, & Kovács (1990) and Moskalik, Buchler, & Marom (1992). These studies were designed to probe the "bump Cepheid" region and hence were essentially limited to stars with $P \lesssim 20^d$. Nonetheless, in the domain of overlap between the present investigation and the earlier work, the results are very similar (see, in particular, Fig. 6 of Moshalik et al. 1992). Since the hydrodynamic codes employed by the two groups are rather different, the similarity of the theoretical light curves is encouraging.

5. DISCUSSION

Figures 1–4 show general trends of slow increase of the Fourier quantities ϕ_{21}, ϕ_{31}, ϕ_{41}, and R_{21} in the domain $P > 20^d$. Compared with the shorter period stars, the scatter is substantial. While there is some indication that observational error may play a large role in this scatter (see § 2 above), it may also be that the Cepheids of long period constitute a more diverse group than do the shorter period stars. Such a possibility is particularly interesting in view of some difficulties in accommodating the long-period Cepheid sample within the framework of standard evolutionary tracks (Simon 1995).

Comparing the observed stars with theoretical calculations, Figures 12–15 show significant discrepancies among the shorter period objects, $P \lesssim 20^d$. This is a reprise of well-known failings of the hydrodynamic models (e.g., Simon 1990b). Among the long-period stars, the considerable observational scatter makes the situation less clear. The models may be more successful in this domain, but a test of this must await a larger, more accurate observational sample such as that now being compiled in MACHO studies of the Large Magellanic Cloud (Cook et al. 1994). In any event, the old dream of using Fourier coefficients to precisely constrain Cepheid parameters still seems a long way from realization.

We are pleased to acknowledge support for this work under the NASA Astrophysical Theory Program, grant NAGW-2395.

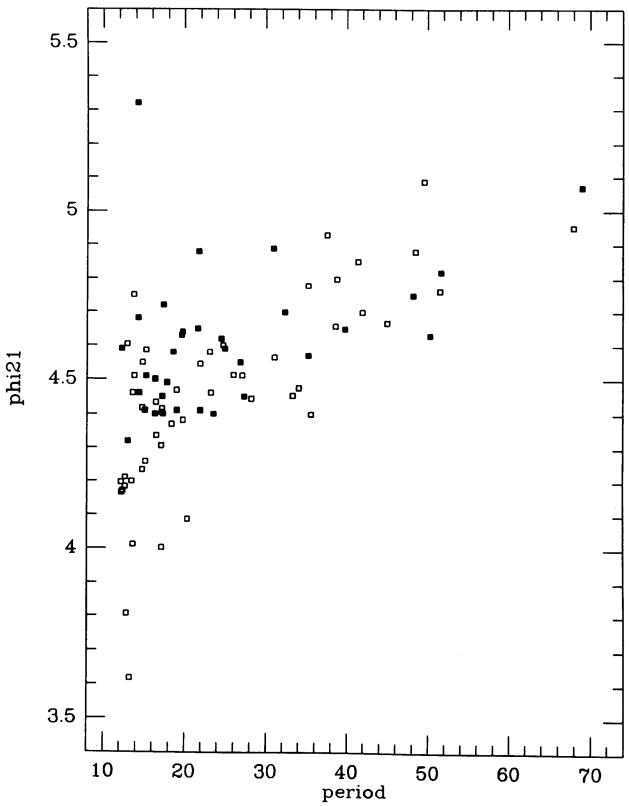

FIG. 12.—ϕ_{21} vs. period: *open squares*: observed stars; *filled squares*: models.

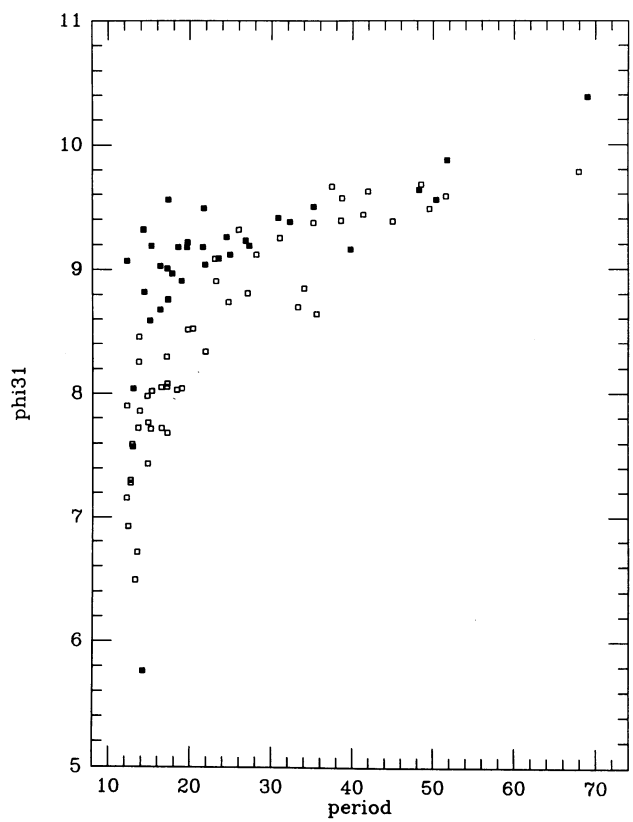

FIG. 13.—ϕ_{31} vs. period. Symbols as in Fig. 12

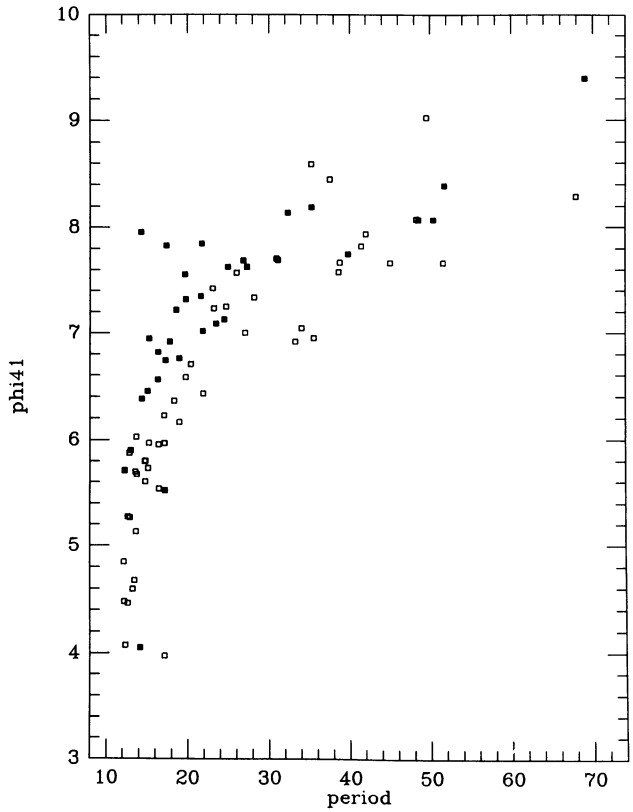

FIG. 14.—ϕ_{41} vs. period. Symbols as in Fig. 12

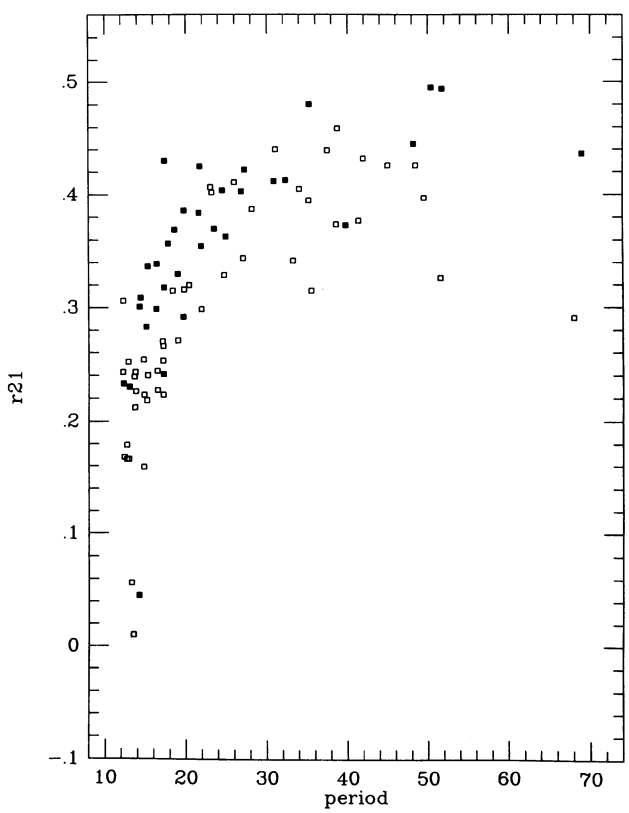

FIG. 15.—R_{21} vs. period. Symbols as in Fig. 12

REFERENCES

Becker, S. A., Iben, I., & Tuggle, R. S. 1977, ApJ, 218, 633
Berdnikov, L. N. 1994, Soviet Astron. Lett., 20, 285
Buchler, J. R., Moskalik, P., & Kovács, G. 1990, ApJ, 351, 617
Chiosi, C. 1989, in The Use of Pulsating Stars in Fundamental Problems of Astronomy, ed. E. G. Schmidt (Cambridge: Cambridge Univ. Press), 19
Cook, K., et al. 1994, in Astronomy Posters (Abstracts) for the 22nd General Assembly of IAU, ed. H. van Woerden (Sliedrecht: Twin Press), 138
Freedman, W. L., et al. 1994, Nature, 371, 757
Kurucz, R. L. 1991, in Precision Photometry, ed. A. G. Davis Phillip, A. R. Upgren, & K. A. Janes (Schenectady: L. Davis Press), 27
Moffett, T. J., & Barnes, T. G. 1985, ApJS, 58, 843
Moskalik, P., Buchler, J. R., & Marom, A. 1992, ApJ, 385, 685
Pel, J. W. 1976, A&AS, 24, 413
Pierce, M. J., et al. 1994, Nature, 371, 385
Saha, A., et al. 1994, ApJ, 425, 14
Simon, N. R. 1990a, MNRAS, 246, 70
———. 1990b, in Confrontation between Stellar Pulsation and Evolution, ed. C. Cacciari & G. Clementini (ASP Conf. Ser. Vol. 11), 193
———. 1995, in Astrophysical Applications of Powerful New Atomic Data Bases, ed. S. J. Adelman & W. L. Wiese (ASP Conf. Ser. Vol. 78), 211
Simon, N. R., & Aikawa, T. 1986, ApJ, 304, 249
Simon, N. R., & Clement, C. M. 1994, ApJ, 419, L21
Simon, N. R., & Lee, A. S. 1981, ApJ, 248, 291
Simon, N. R., & Moffett, T. J. 1985, PASP, 97, 1078
Simon, N. R., & Schmidt, E. G. 1976, ApJ, 205, 162